Iraqi Journal of Physics, 2019 *Vol.17, No.43, PP. 33-40*
DOI: 10.20723/ijp.17.43.33-40

Fabrication of electroluminescence device for PEDOT: PSS / ploy TPD/Eu_2O_3 nanoparticles junction

Hussein Riyadh Mohammed and Omer A. Ibrahim
Department of Physics, College of Science, University of Baghdad
E-mail: hussieni6762@gmail.com

Abstract

The nanoparticles light emitting diode (NPs-LED) fabricated for organic and inorganic semiconductors to achieve electroluminescence (EL). The nanoparticles of Europium oxide(Eu_2O_3) were incorporated into the thin film layers of the organic compounds, poly(3,4,- ethylene dioxythiophene)/polystyrene sulfonic acid (PEDOT:PSS), N,N'–diphenyl-N,N' –bis(3-methylphenyl)-1,1'-biphenyl 4,4'- diamine (poly TPD) and polymethyl methacrylate (PMMA), by the spin coating and with the help of the phase segregation method. The EL of NPs-LED, was study for the different bias voltages (20, 25, 30) V at the room temperature, from depending on the CIE 1931 color spaces and it was generated the white light at 20V, the orange light generation at 25Vand the red light at 30 V. That by benefit from transition between deep levels in energy gap for Eu_2O_3 nanoparticles (surface state) and magnetic dipole states for Eu^+ ($^5D_{0-3}$ and$^5L_6$ to $^7F_{0-6}$). The Current – Voltage (I-V) Behavior demonstrate that the current comparative with the voltage was good and the knee voltage was 5 V. The EL spectrum shows a broad band emission, the range from EL 485-700 nm. Finally, the range of correlated color temperature (CCT) it was between (1200 to 4000).

Key words
Europium oxide, nanoparticle, electroluminescence, light-emitting diode.

Article info.
Received: Aug. 2019
Accepted: Oct. 2019
Published: Dec. 2019

تصنيع نبائط الأستضائية الكهربائية هجينة المفرق من PEDOT:PSS / بولمر TPD/ جسيمات Eu_2O_3 النانوية

حسين رياض محمد و عمر عدنان ابراهيم
قسم الفيزياء، كلية العلوم، جامعة بغداد

الخلاصة

تم تصنيع الصمام الثنائي الباعث للجسيمات النانوية (NPs-LED) لأشباه الموصلات العضوية وغير العضوية لتحقيق الاستضائية الكهربائية (EL). حيث تم غرس الجسيمات النانوية لأكسيد اليوروبيوم (Eu_2O_3) في طبقات الأغشية الرقيقة للمركبات العضوية المتكونة من، poly(3,4,- ethylene dioxythiophene) N,N'–diphenyl-N,N' –bis(3-methylphenyl)-1,1'-biphenyl 4,4'- diamine(TPD) (PDOT:PSS) / (PMMA): بواسطة الطلاء الدوار و بمساعدة طريقة الفصل الطوري. تم دراسة الاستضائية الكهربائية للدايود الباعث للضوء، بتطبيق جهود انحياز مختلفة (20، 25، 30) فولت في درجة حرارة الغرفة، ومن أخذ مساقط الالوان على مخطط المساحات اللونية CIE 1931، لوحظ توليد الضوء الأبيض عند 20 فولت، وتوليد الضوء البرتقالي في 25 فولت و الضوء الأحمر في 30 فولت. وفسر الحصول على هذهِ الألوان من الانتقالات بين المستويات العميقة في فجوة الطاقة للجسيمات النانوية للاوكسيد اليوريبيوم (المستويات السطحية) وحالات ثنائي القطب المغناطيسي. ($5D_{0-3}$,$5L_6$ - $7F_{0-6}$) Eu^+. كذلك يتضح سلوك التيار- الجهد (I-V) أن التيار المقابل للجهد كان جيدًا وأن جهد العتبة كان 5 فولت. من مخطط الاستضائية الكهربائية يظهر طيف انبعاث واسعاً يتراوح من (480-700) نانومتر. أخيرًا، تتراوح درجة حرارة المرتبطة باللون (CCT) بين (1200 إلى 4000).

Introduction

Due to its excellent chemical and physical properties, rare earth compounds (oxides) have great interest research for many years and are now widely applied in many fields, for example: fluorescent devices, catalysts and fuel cells [1]. Europium oxide (Eu_2O_3) is the rare earth oxides and is that very attractive because of its wide band gap about 3.7 eV, high dielectric constant and outstanding characteristics of large displacement of the conduction band [2]. Recently, Eu_2O_3 has been studied and used in various new devices, like optical devices, microelectronics and telecommunications [3]. The benefits of the unique rare earth oxide, Eu_2O_3 has a different model of the energy zone from other semiconductors, which includes the conduction band, valence band and extremely narrow 4f group [4]. L al et al. reported that the "relative position of the 4f band has a significant effect on genesis of charge carriers. They presented the unoccupied f-levels of Eu_2O_3 lie in the forbidden zone and occupied f levels lie outside the gap. In this case, the preferred energy Process will be the excitation of electrons from valence O2p band goes to unoccupied f levels below conductivity lane, leading to the 4f - 4f intra-atomic transition [5]. Therefore, in terms of the type of semiconductor material, Eu_2O_3 may show a number of characteristic lines of Eu^{3+}, It have deep sub levels ($^5D_0 \rightarrow {}^7F_{0, 1, 2, 3 \text{ and } 4}$) in Eu_2O_3 Resulting from the splitting of spectrum lines known as the effect of stark on the atom or partial because of the occurrence under the influence of an external electric field rather than wide inter zone transition [6].

Experimental work

Prepared and manufactured the hybrid film (ITO/PEDOT: PSS/TPD: PMMA/ Eu_2O_3/Alq_3/AL) in several stages, will summarize the following steps:

a) Filtered the PEDOT: PSS compound by 0.45 µm PES filter into an amber vial and saved the product in a bottle approved because of the impact of the compound for light The ITO glass was deposited a layer of PEDOT: PSS in the spin coating machine by speed 1000 rpm for 30 s and then dry the film by oven at 120° C for 15 minutes.

b) Dissolved 70 mg of TPD in 2 ml of chloroform and mixed it well. Then added 2:1 of PMMA and took the weight of the mixture, after that add weight of 0.05 % from Europium oxide. The good we deposited these organic compounds and nanoparticles on the layer (PEDOT:PSS) by the spin coating at 30 s in speed 2500 rpm, to complete the drying, the film was put in the oven at 60 ^oC for 1h to get rid of solvents suspended, the layers of the device was content ITO/PEDOT:PSS /TPD:PMMA / Eu_2O_3.

c) Dissolved 70 mg of Alq_3 in 3 ml of ethanol and mixed it well by hot pleat magnetic stirrer, the solution was deposited by the spin coating machine at 30 s in speed 2500 rpm and put the films in the oven at 60 ^oC for 1 h to get rid of solvents suspended, finally, deposited the electrodes. Four layers ready to take the necessary measurements (ITO/PEDOT:PSS /TPD:PMMA / Eu_2O_3/ALq_3/AL) as Fig.1.

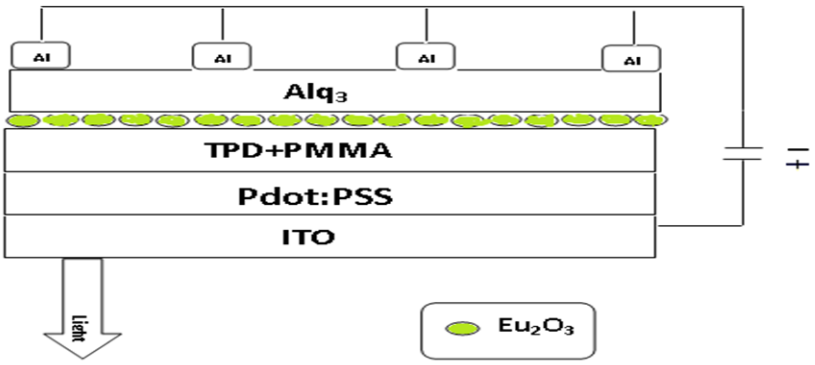

Fig.1: Stricture of device PEDOT:PSS/TPD:PMMA/Eu_2O_3/Alq_3.

Results and discussion

1. Hall Effect

The Hall Effect measurement was studied by the Ecopia HMS-3000 Hall measurement system. The Eu_2O_3 NPs film was electrically characterized using Hall Effect measurement. The film of 600 nm thickness shows semiconductor behavior of n-type conductivity. The conductivity and resistivity values were 1.584X10^{-4} $(\Omega\ cm)^{-1}$ and 6.315X10^{3} $(\Omega\ cm)$ respectively, while the mobility was 6.292 X 10^{2} $(cm^2/V\ sec)$. All the parameters are tabulated in Table 1.

Table 1: Hall measurement for Eu_2O_3.

Samp.	Hall Coefficient (m^2/C)	Conductivity $(\Omega.cm)^{-1}$	Bulk Concentration $(cm)^3$	Mobility (cm^2\V.s)	Resistivity (Ω.cm)
Eu_2O_3	1.584 X10^{-4}	1.584 X10^{-4}	-1.571 X10^{+12}	6.292 X^{10+2}	6.315X10^{3}

2. Current- Voltage characteristics

The current–voltage (I-V) characteristics of the hybrid junction ITO/PEDOT: PSS/TPD: PMMA/Eu_2O_3/Alq_3/Al device as function of the bias voltage at dark and room temperature shown in Fig.2, and it clarifies that the current transport mechanism it will be seen in three different regions.

The current in region 1 (<5 V) a linear relationship vs. the voltage, that is (IαV). This indicates that tunneling at low voltages prevails in the traffic flow. The boundary for this area was determined below the knee tension.

In region 2 (5-20 V), the current increases exponentially as (Iα exp (V)) carriers injected into the dielectric are generated as a result of a thermionic process flowing through the barrier. As a result, the number of trapped charges is much bigger than the number of free charges, and shows the relation between the bias voltage and current was exponential [7].

With further application of voltage, the injected carriers quickly increase and the traps are filled (the traps state are $^5D_0$, $^5D_1$, $^5D_2$, $^5D_3$, $^5L_6$, NPs state and defect stated) [3] in 20V it was names Traps-Filled-Limit Voltage (V_{TFL}).

Finally above 20V region 3 (above 20 V) shows the power relationship between the bias voltage and current ($I\alpha V^2$), the light emission started at region (3), in 20V and 610 µm, because the transport through the ITO/PEDOT:PSS/TPD: PMMA/Eu_2O_3/Alq_3/Al. The emission from the hybrid film it was by the trapped charge limited current phenomena (TCLC) in the band gap of the Eu_2O_3 NPs, This means that when the density of injected free charge carriers is much greater than the thermally generated free charge carriers, the SCLC conductivity should be dominant [8].

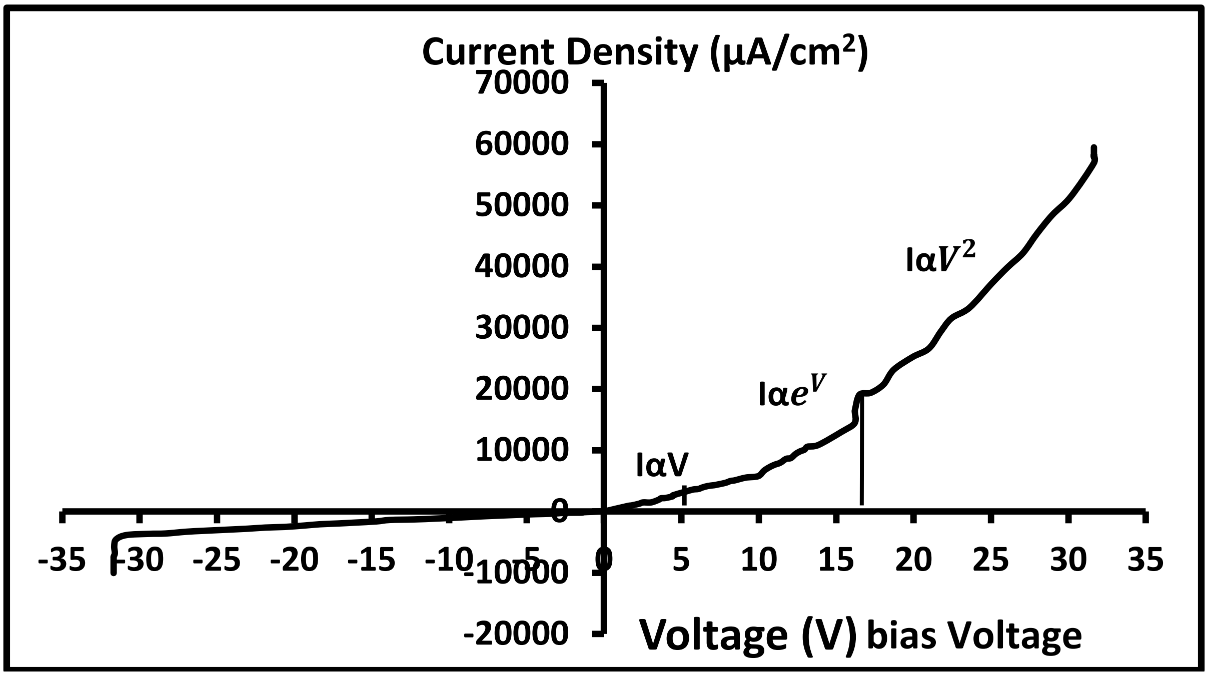

Fig.2: I-V characteristics of Eu_2O_3 hybrid film.

With expanding forward inclination, the float current streaming in the inverse bearing doesn't rely on upon. The possibility obstruction stature What's more will improve those electrons stream from those n-(NPs) of the p-(TPD) Also. Gaps from those p-(TPD) of the n-(NPs). The progressive recombination might provide for climb of the head inclination present stream. This implies that those diode imperviousness might firstly diminish upon the. Increment of the a head segregation racial inclination voltage (i. E., the bringing down of the barrier). The semi-log plot of the I-V. Information In RT will be demonstrated to Fig.3 What's more it illustrates that the current transport system will be exhibited to three diverse districts.

3. Electroluminesces measurements

The electroluminescence at a bias voltage of 25 voltages, the spectrum of the light that was obtained from the hybrid junction device (PEDOT: PSS/TPD: 1PMMA: 0.5 wt. % Eu_2O_3: Alq_3) as shown in Fig.4 and shows a broad band emission (480-700) nm. A layer of (PEDOT: PSS) it was added to increase carrier transport due to its high conductivity [9], and the transport layers of the carrier in our hybrid device, the TPD for holes transfer and Alq3 for electrons transfer. The holes are injected by the ITO anode in the HOMO of the TPD. It was then transferring to V.B or $^7F_0$, $^7F_{1.2}$, $^7F_{3.4}$ and $^7F_{5.6}$ Eu_2O_3. At the same time, the electrons transport through from the cathode to the LOMO of Alq_3 and transport to the conduction band (C.B) or ($^5D_0$, $^5D_1$, $^5D_2$, $^5D_3$, $^5L_6$ and the surface states of QDs) of the Eu_2O_3 [2], as shown in Fig. 3. Subsequently, holes and electrons in NPs Eu_2O_3 are also recombined as excitoins, also known as inter band recombination. It is the process of recombining holes and electrons through trap states (surface state for Eu_2O_3 NPs and magnetic dipole transition for Eu+ [$^5D_{0-3}$ and $^5L_6$ to $^7F_{0-6}$]) to produce light at different wavelengths. A process that involves recombination by defects is called Shockley-Reed-Hall recombination [10, 11]. In Fig.4 the Notable peak Stretching from orange 585nm to red emission around 650 nm is related to ($^5D_0$) to ($^7F_0$ and $^7F_{1,2}$).

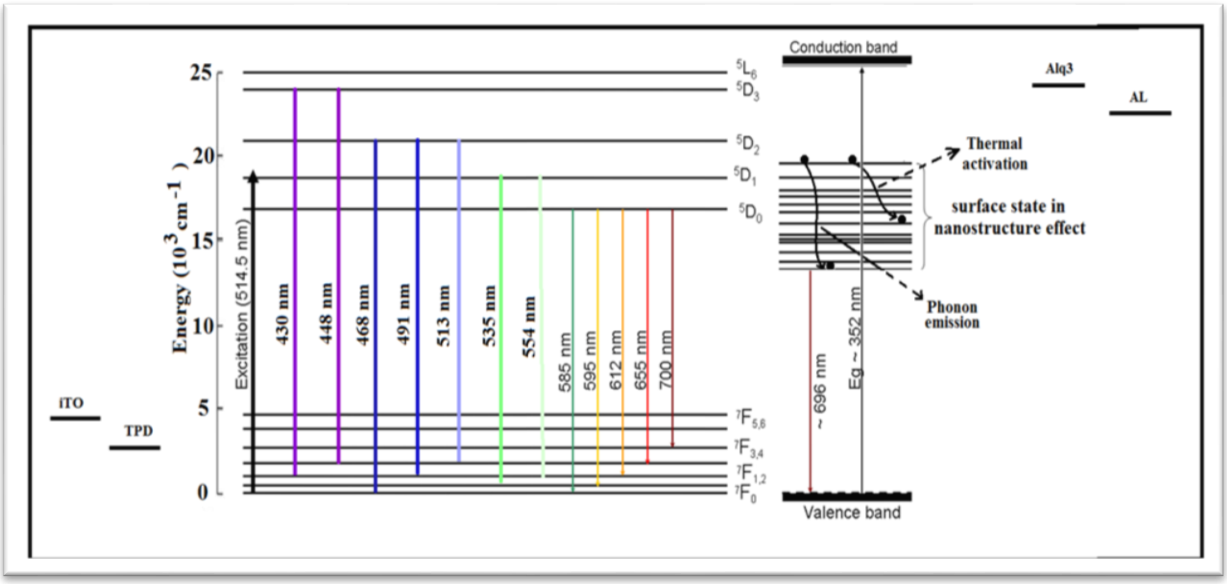

Fig.3: ITO/TPD: PMMA/Eu_2O_3/Alq_3/Al hybrid device demonstrating energy bands diagram [3, 4, 12 and 13].

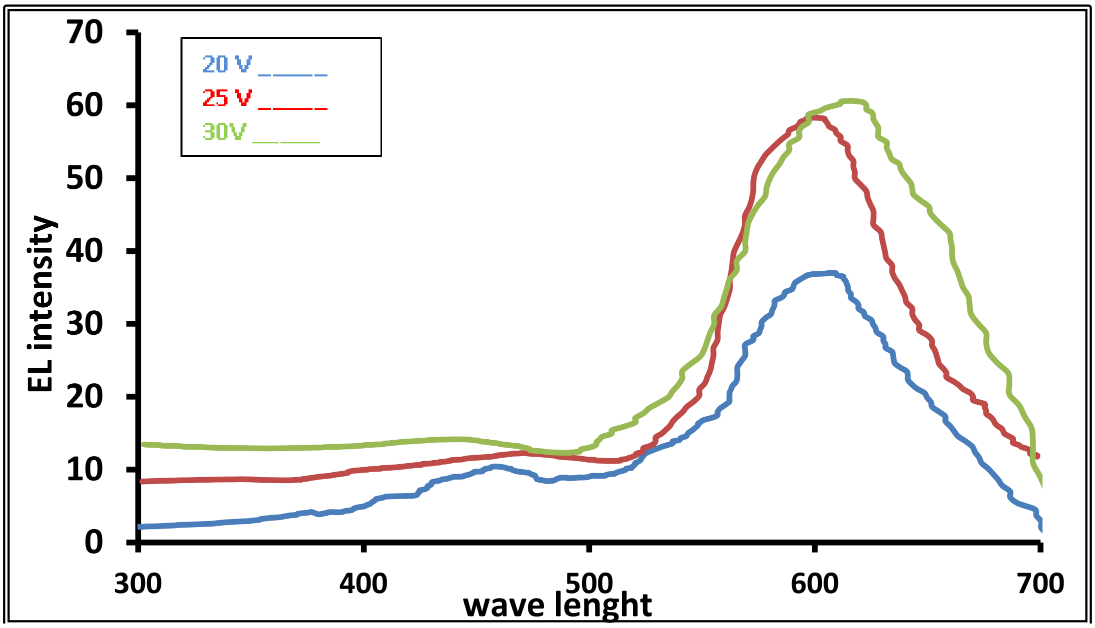

Fig. 4: EL of PEDOT:PSS/TPD:PMMA/Eu_2O_3/Alq_3 at different voltage.

The common transitions in the Eu_2O_3 NPs can be briefly in Fig.3:
The violet emission at ≈360nm is due to the band to band transition [3]. The blue emission of 430 nm to the blue emission of 513 nm corresponds to the transitions ($^5D_3$ and $^5D_2$) to ($^7F_0$, $^7F_2$ and $^7F_3$) [11]. The EL peak 410nm corresponds to the emission of TPD, because the band gap of TPD is 3 eV [6]. These peaks appear when using NPs where an Auger-assisted energy due to nano size materials which cause high Auger recombination cross section. With a decrease in TPD, the number of injected holes through the interface NP TPD / Eu_2O_3 decreased, while the electrons are efficiently injected in to the C.B of the Eu_2O_3 NPs [14]. The excitations via nan-radiative energy transfer from the TPD to the Eu_2O_3 NPs because EL device structures with sub-10nm separation between TPD and Eu_2O_3 NPs [15]. By observing the energy bands diagram of Europium Oxides, the emissions from sub-levels of 520 to 700 nm dominated, causality the green emission 520 nm corresponds to ($^5D_1$ and $^5D_0$) to ($^7F_0$ and $^7F_{1,2}$) transitions [3, 12]. The orange 585 nm to red emission around 700 nm is related to ($^5D_0$) to ($^7F_0$, $^7F_{1,2}$ and $^7F_{3,4}$) transitions or surface state in nanostructure effect to V.B of Eu_2O_3[3]. All these transitions are appearing in Fig.5 As illustrated Fig.5. The color of light is located by the CIE 1931 Chromaticity Coordinate. The Chromaticity Coordinates x y on CIE 1931 Chromaticity Coordinate is found from

$$x = \frac{X}{X+Y+Z} \quad (1)$$

$$y = \frac{Y}{X+Y+Z} \quad (2)$$

where the X, Y and Z are area under the curve for red, green and blue are regions in EL spectrum, respectively.
The CCT of light can be found by using McCamy's approximation polynomial to estimate the CCT from the x and y chromaticity coordinates as in Eq. (3) [13]:

$$CCT = -449n^3 + 3525n^2 - 6823n + 5520.33 \quad (3)$$

where

$$n = (x - 0.332)/(y - 0.1855) \quad (4)$$

The all result can be tabulated in Table 2.

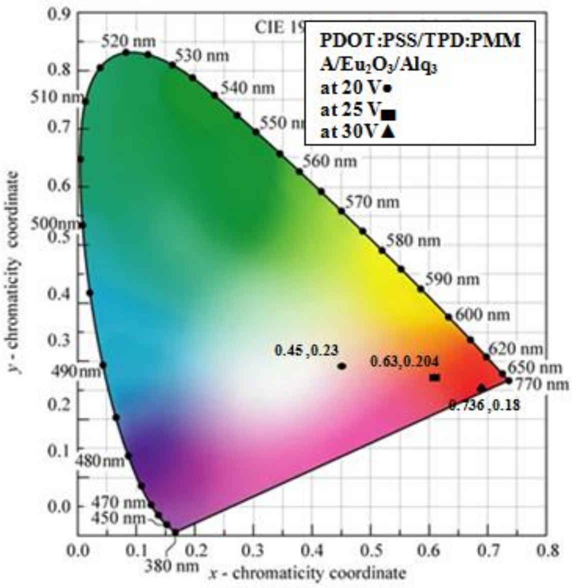

Fig.5: Coordinates of the hybrid devices in the CIE 1931 chromaticity diagram.

Table 2: CCT and xy coordinates for different bias voltage.

Simple	Bias voltage (V)	x,y	CCT (K)
ITO/PEDOT:PSS/TPD: PMMA/Eu_2O_3/Alq_3/Al	20	0.45,0.23	3880
	25	0.63,0.2	1410
	30	0.73,0.18	1280

Fig. 5: For the light generation ITO/PEDOT:PSS/TPD: PMMA/Eu_2O_3/Alq_3/Al hybrid.

Conclusions

From the summarizing result, we demonstrate the possibility of manufacturing an EL Device that generates a multi-color control of the bias voltage, which is advantageous from the transition between a deep level in the Eu_2O_3 NP ($^5D_{0-3}$ and $^5L_6$ to $^7F_{0-6}$) forbidden zone and Eu_2O_3 NP defect states. The generation of white light is explained by an increase in the bias voltage, as the number of transitions between deep Eu_2O_3 levels increases

References

[1] Abdoulaye Diallo, Bakang M. Mothudi, Elayaperumal Manikandan, Malik Maazaa, J. Nanophoton., 10, 2 (2016) 1-12.

[2] Yuen Yung Hui, Chun-Yu Lee, and Ching-Fuh Lin, Proceedings of the 7th IEEE International Conference on Nanotechnology, Hong Kong, (2007) 862-865.

[3] Rachna Ahlawat, International Journal of Advance Research in Science and Engineering, 6, 6 (2017) 590-597.

[4] G. Wakefield, H. A. Keron, P. J. Dobson, J. L. Hutchison, Journal of Colloid and Interface Science, 215, 1 July (1999) 179-182.

[5] Xue Yin, Shenwei Wang, Guangyao Mu, Guangmiao Wan, Miaoling Huang, Lixin Yi, Journal of Physics D: Applied Physics, 50, 10 (2017) PP.

[6] S.A. Lourenco, N.O. Dantas, E.O. Serqueira, W.E.F. Ayta, A.A. Andrade, M.C. Filadelpho, J.A. Sampaio, M.J.V. Bell, M.A. Pereira-da-Silva, Journal of Luminescence, 131 (2011) 850-855.

[7] Zubair Ahmad, P.C. Ooi, K.C. Aw, M.H. Sayyad, Solid State Communications, 151 (2011) 297-300.

[8] Zubair Ahmad and Muhammad H. Sayyad, Physica E, 41 (2009) 631-634.

[9] Atsushi Nitta, Kazuki Shimono, Advances in Materials Physics and Chemistry, 5 (2015) 467-476.

[10] Thierry Goudon, Vera Miljanovic, Christian Schmeiser, Society for Industrial and Applied Mathematics, 67, 4 (2007) 1183-1201.

[11] Ijaz Hussain, Nargis Bano, Sajjad Hussain, Yousuf Soomro, Omer Nur, Magnus Willander, Materials, 4 (2011)

1260-1270.
[12] Kohei Yoshimoto, Yoshinobu Ezura, Motoi Ueda, Atsunobu Masuno, Hiroyuki Inoue, Masafumi Mizuguchi, Opt. Lett., 44, 4 (2019) 875-878.
[13] Omar Adnan Ibrahim, "White light generation" LAP LAMBERT Academic publishing, (2017).
[14] Lei Qian, Ying Zheng, Kaushik R. Choudhury, Debasis Bera, Franky So, Jiangeng Xue, Paul H. Holloway, Nano Today, 5 (2010) 384-389.
[15] Oleksii Kopylov, "Hybrid Light-Emitting Diode Enhanced with Emissive Nanocrystals", Thesis, Technical University of Denmark in Denmark, (2013).